ATP Interaction with the Open State of the K_{ATP} Channel

D. Enkvetchakul,* G. Loussouarn,† E. Makhina,† and C. G. Nichols†
*Division of Renal Medicine and †Department of Cell Biology and Physiology, and Washington University School of Medicine, St. Louis, Missouri 63110 USA

ABSTRACT The mechanism of ATP-sensitive potassium (K_{ATP}) channel closure by ATP is unclear, and various kinetic models in which ATP binds to open or to closed states have previously been presented. Effects of phosphatidylinositol bisphosphate (PIP_2) and multiple Kir6.2 mutations on ATP inhibition and open probability in the absence of ATP are explainable in kinetic models where ATP stabilizes a closed state and interaction with an open state is not required. Evidence that ATP can in fact interact with the open state of the channel is presented here. The mutant Kir6.2[L164C] is very sensitive to Cd^{2+} block, but very insensitive to ATP, with no significant inhibition in 1 mM ATP. However, 1 mM ATP fully protects the channel from Cd^{2+} block. Allosteric kinetic models in which the channel can be in either open or closed states with or without ATP bound are considered. Such models predict a pedestal in the ATP inhibition, i.e., a maximal amount of inhibition at saturating ATP concentrations. This pedestal is predicted to occur at >50 mM ATP in the L164C mutant, but at >1 mM in the double mutant L164C/R176A. As predicted, ATP inhibits Kir6.2[L164C/R176A] to a maximum of ~40%, with a clear plateau beyond 2 mM. These results indicate that ATP acts as an allosteric ligand, interacting with both open and closed states of the channel.

INTRODUCTION

First described in 1983 by Akinori Noma, ATP-sensitive potassium (K_{ATP}) channels are reversibly inhibited by the nonhydrolytic binding of intracellular ATP (Noma, 1983; Ashcroft, 1988; Nichols and Lederer, 1991). The K_{ATP} channel is a hetero-octamer formed by an inward-rectifying K^+-channel subunit (Kir6.x) and a sulfonylurea receptor (SURx) (Aguilar-Bryan et al., 1995; Inagaki et al., 1995, 1996) in a 4:4 stoichiometry (Clement et al., 1997; Inagaki et al., 1997; Shyng and Nichols, 1997). ATP inhibition occurs through interaction with the Kir6.2 subunit (Shyng et al., 1997a; Tucker et al., 1997, 1998; Tanabe et al., 1999), whereas the SURx subunit confers high-affinity block by sulfonylureas and stimulation by K^+ channel openers and MgADP (Aguilar-Bryan et al., 1995; Inagaki et al., 1996; Isomoto et al., 1996; Nichols et al., 1996; Gribble et al., 1997a,b; Shyng et al., 1997b; Schwanstecher et al., 1998).

Although there are a few mutations that alter ATP sensitivity without affecting the channel gating in the absence of ATP (Tucker et al., 1997; Li et al., 2000), most mutations in the Kir6.2 subunit alter sensitivity to ATP inhibition ($K_{1/2,ATP}$) and open probability in the absence of ATP (P_{Ozero}) in a strongly correlated manner. This correlation can be quantitatively explained by models that assume ATP binds to the closed state of the channel (Shyng et al., 1997a; Enkvetchakul et al., 2000). In accord with this notion, open-time distributions are generally not altered in the presence of ATP (Alekseev et al., 1998; Drain et al., 1998; Trapp et al., 1998; Enkvetchakul et al., 2000; Li et al., 2000), and diverse steady-state and kinetic nucleotide sensitivity data of wild-type and mutant K_{ATP} are reproducible by such a gating scheme (Enkvetchakul et al., 2000).

Developing appropriate gating schemes to describe K_{ATP} channel nucleotide sensitivity is of more than esoteric interest. An understanding of state interactions will require incorporation into future structural models of K_{ATP} channel activity. The possibility of a fully allosteric gating scheme in which channels can be open or closed, regardless of ligand binding, was briefly considered (Enkvetchakul et al., 2000), but in the absence of concrete evidence for ATP interaction with the open state, such a model need not be invoked. The acceptance of cyclic nucleotides as allosteric ligands for cyclic nucleotide-gated (CNG) channels ultimately required demonstration that ligand-independent openings are possible in the absence of nucleotides (Tibbs et al., 1997). Conversely, proof of ATP interaction with the K_{ATP} channel open state ultimately requires demonstration of opening in the presence of saturating [ATP]. We now show clear evidence that ATP can interact with the open state of K_{ATP} channels. At a concentration that has no discernable inhibition of channel activity, ATP abolishes Cd^{2+} sensitivity of Kir6.2[L164C] + SUR1 (164C) channels. In the double mutant Kir6.2[L164C, R176A], a clear plateau is observed in the maximum ATP inhibition. An allosteric gating scheme can account for the above data, as well as the behavior of wild-type and other mutant channels, by appropriate shifts in closed-open equilibrium constants. In wild-type and low-open-state stability mutants, however, occupancy of the ATP-liganded open state becomes negligible. For these channels, the appropriate schemes then reduce to ones in which ATP accesses only the closed state.

Received for publication 23 August 2000 and in final form 8 November 2000.

Address reprint requests to Dr. C. G. Nichols, Department of Cell Biology and Physiology, Washington University School of Medicine, 660 South Euclid Avenue, St. Louis, MO 63110. Tel.: 314-362-6630; Fax: 314-362-7463, E-mail: cnichols@cellbio.wustl.edu.

0006-3495/01/02/719/10 $2.00

MATERIALS AND METHODS

Molecular biology

Constructs containing point mutations were prepared by overlap extension at the junctions of the relevant residues by sequential polymerase chain reaction (PCR). Resulting PCR products were subcloned into pCMV6b vector and sequenced to verify the correct mutant construct, before transfection. Mutations in Kir6.2 were constructed in the background construct of Kir6.2[N160D, C166S] described previously (Loussouarn et al., 2000). The N160D mutation allows measurement of zero current in the presence of the pore blocker spermine (Shyng et al., 1997a), and the C166S mutation removes a native cysteine that can react with cadmium.

Expression of K_{ATP} channels in COSm6 cells

COSm6 cells were plated at a density of $\sim 2.5 \times 10^5$ cells per well (30-mm six-well dishes) and cultured in Dulbecco's modified Eagle medium plus 10 mM glucose (DMEM-HG), supplemented with fetal calf serum (FCS, 10%). The following day, cells were transfected by incubation for 4 h at 37°C in DMEM containing 10% Nuserum, 0.4 mg/ml diethylaminoethyl-dextran, 100 μM chloroquine, and 5 μg each of pCMV6b-Kir6.2 or mutations, pECE-SUR1, and pECE-GFP (green fluorescent protein) cDNA. Cells were subsequently incubated for 2 min in phosphate-buffered salt solution containing DMSO (10%) and returned to DMEM-HG plus 10% FCS. Cells were assayed for K_{ATP} currents by patch-clamp measurements 2–4 days after transfection.

Patch-clamp measurements

Patch-clamp experiments were made at room temperature in a chamber that allowed rapid change of the solution bathing the exposed surface of the isolated patch. Micropipettes were pulled from thin-walled glass (WPI Inc., New Haven, CT) on a horizontal puller (Sutter Instrument Co., Novato, CA). Electrode resistance was typically 0.5–2 MΩ (~5 MΩ for single-channel currents) when filled with K-INT or KF-INT solution (see below). Membrane patches were voltage clamped with an Axopatch 1D patch clamp (Axon Inc., Foster City, CA). For ATP dose-response experiments, the bath (intracellular) and pipette (extracellular) solutions (K-INT) had the following composition: 140 mM KCl, 10 mM K-HEPES, 1 mM K-EGTA, pH 7.3. For experiments using Cd^{2+}, the bath (intracellular) and pipette (extracellular) solutions (KF-INT) had the following composition: 120 mM KCl, 20 mM KF, 10 mM K-HEPES, pH 7.3. In these experiments using Cd^{2+}, EGTA was omitted because of Cd^{2+} chelation, and 20 mM KF was used as a replacement for Ca^{2+} chelation. All currents were measured at a membrane potential of −50 mV (pipette voltage = +50 mV). Inward currents at this voltage are shown as upward deflections. Data were normally filtered at 0.5–20 kHz (10–20 kHz for single channel), signals were digitized at 88 kHz (Neurocorder, Neurodata, New York, NY) and stored on videotape or digitized and stored directly to computer/hard drive using Clampex software (Axon). Tape-recorded experiments were digitized into a microcomputer using Axotape, Fetchex, or Clampex software (Axon). Off-line analysis was performed using Fetchan, pSTAT (Axon), and Microsoft Excel programs. Single-channel recordings were re-filtered using a digital Gaussian filter at 3 kHz through Fetchan and analyzed using the half-amplitude threshold criteria to create idealized records. A dead time (t_d) of 100 μs was enforced on the idealized records by ignoring events less than t_d and concatenating dwell times with neighboring events, which is required by the missed events correction described below. Wherever possible, data are presented as mean ± SEM.

Model simulations

Aggregated, continuous-time Markov models were assumed to be representative of actual K_{ATP} channel kinetics and were used for simulations. The channel was assumed to have four independent and kinetically identical subunits, with the channel being open only if all four subunits were in the open state. Rate constants between states were constrained as multiples of individual subunit rate constants depending on the number of subunits available to make a given transition. Microreversibility was observed. A rate matrix **Q** was constructed, and probability density functions were calculated using matrix mathematics as described by Colquhoun and Hawkes (1995). Matrix **Q** was constructed with each element (i, j) equal to the rate constant from state i to state j, and elements (i, i) were set equal to the negative sum of all the other values in that row. Closed states (m in number) and open states (n in number) were grouped to allow partitioning of the **Q** matrix into submatrices ($\mathbf{Q_{AA}}$, $\mathbf{Q_{AB}}$, $\mathbf{Q_{BA}}$, $\mathbf{Q_{BB}}$), representing the transition rates from closed to closed, closed to open, open to closed, and open to open states, respectively. A first-order correction for missed events (Qin et al., 1996) was applied to probability density functions (PDFs). For the calculation of closed PDFs, adjusted matrices ($^e\mathbf{Q_{AA}}$ and $^e\mathbf{Q_{AB}}$) were defined as follows:

$$^e\mathbf{Q_{AA}} = \mathbf{Q_{AA}} - \mathbf{Q_{AB}}(\mathbf{I} - \exp(\mathbf{Q_{BB}}t_d))\mathbf{Q_{BB}}^{-1}\mathbf{Q_{BA}} \quad (1)$$

$$^e\mathbf{Q_{AB}} = \exp[t_d\mathbf{Q_{AB}}(\mathbf{I} - \exp(\mathbf{Q_{BB}}t_d)\mathbf{Q_{BB}}^{-1}\mathbf{Q_{BA}}]\mathbf{Q_{AB}}, \quad (2)$$

where t_d is the dead time, i.e., the minimum duration of an event that will be detected, and **I** is the identity matrix. Closed PDFs were then calculated using Eq. 3:

$$\mathrm{PDF}_{\mathrm{closed}}(t) = \mathbf{\Phi}_c\exp(t\,^e\mathbf{Q_{AA}})(^e\mathbf{Q_{AB}})\mathbf{u}_B, \quad (3)$$

where $\mathbf{\Phi}_c$ is a $1 \times m$ row vector containing the probabilities of starting a closed event in each closed state, and $\mathbf{u}_B$ is an $m \times 1$ column vector whose elements are all 1. Open PDFs were calculated in similar fashion.

The task of determining all unique states, calculating rate constants, and building the **Q** matrix was carried out using Microsoft Excel. Matrix operations were performed either with MathCad6 (MathSoft, Cambridge, MA) or with original programs written in Visual Basic or Visual Basic for Applications (Microsoft, Redmond, WA). The matrix exponential was calculated using either spectral expansion of a matrix or by the Taylor series expansion of an exponential (Colquhoun and Hawkes, 1995a,b).

RESULTS

ATP prevents cadmium block and unblock in Kir6.2[L164C] + SUR1

Residue 164 lines the channel pore in the M2 helix of the Kir6.2 subunit (Loussouarn et al., 2000); mutant Kir6.2[L164C] + SUR1 (L164C) channels are inhibited by micromolar concentrations of cadmium, due to coordination by the thiol moieties of the cysteines at position 164 (Loussouarn et al., 2000). L164C channels have a very high open probability with very low ATP sensitivity (Enkvetchakul et al., 2000; see Fig. 3). Fig. 1 *A* demonstrates that 1 mM ATP causes essentially no inhibition of L164C, but 10 μM Cd^{2+} reversibly blocks the channel. In the same patch, despite no inhibitory effect of 1 mM ATP on L164C channels, the application of ATP before cadmium exposure completely prevents block by cadmium (Fig. 1 *A*). If cadmium is applied first, the subsequent application of 1 mM ATP prevents inhibition of further channels by cadmium (Fig. 1 *B*). Even more striking, channel opening after removal of cadmium can be halted by the application of ATP (Fig. 1 *C*). Although ATP causes no inhibition at this concentration, it

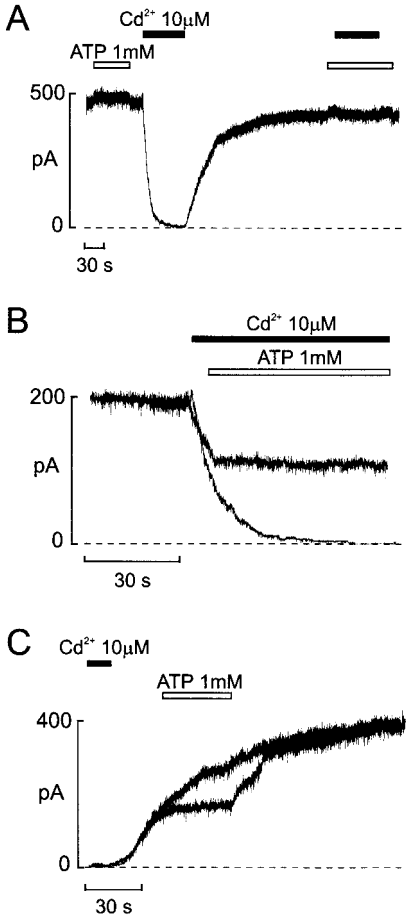

FIGURE 1 ATP prevents cadmium block and unblock of Kir6.2[L164C] + SUR1 (L164C) channels. Representative currents were recorded from inside-out membrane patches at −50 mV with KF-INT solutions (see Materials and Methods). In this and all subsequent figures, inward currents are shown as upward deflections. (*A*) Recording of a single patch with L164C exposed to 1 mM ATP or 10 μM Cd^{2+} as indicated; (*B* and *C*) Recording of L164C exposed to 10 μM Cd^{2+} alone, overlaid on recording of L164C exposed to both 10 μM Cd^{2+} and 1 mM ATP as indicated.

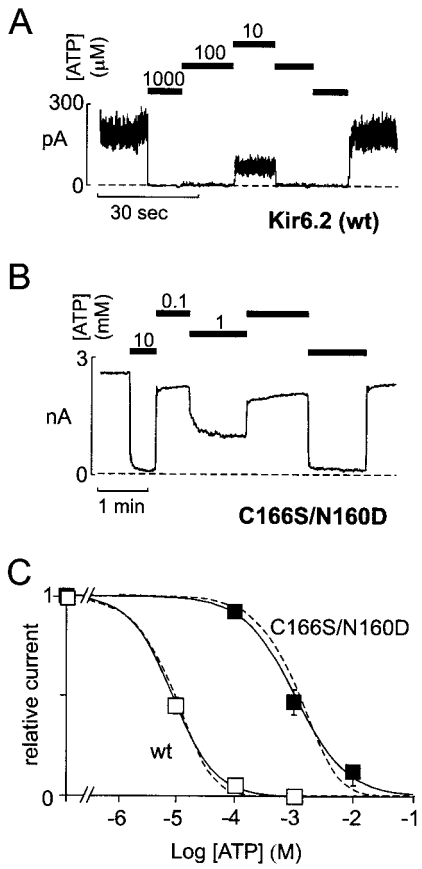

FIGURE 2 ATP sensitivity of Kir6.2 + SUR1 (wt) and of the background mutant Kir6.2[C166S, N160D] + SUR1 (C166S/N160D) channels. (*A* and *B*) Representative recordings were made from inside-out membrane patches at −50 mV with K-INT solution (see Materials and Methods). ATP was applied where indicated. (*C*) [ATP]-response relationship of wt (□) and C166S/N160D (■). Solid curves are Hill plots; dashed lines are from simulations of model III (see text).

appears to stabilize channels such that if open, Cd^{2+} cannot bind, or if Cd^{2+} is already bound, it cannot unbind. That ATP causes no inhibition of the channel but can prevent cadmium block and unblock indicates an action of ATP on the open state of L164C.

A plateau of ATP inhibition in L164C/R176A

Wild-type K_{ATP} channels, formed of Kir6.2 + SUR1 subunits, are very sensitive to ATP, being half-maximally inhibited at ~10 μM (Fig. 2 *A* and *C*; Inagaki et al., 1996). The mutations considered below were generated in the background of Kir6.2[C166S, N160D] (166S/160D). Expression of C166S/N160D + SUR1 generates channels that are considerably less sensitive to ATP than wild type, but which are nevertheless still apparently completely inhibited by high millimolar [ATP] (Fig. 2, *B* and *C*; Trapp et al., 1998; Loussouarn et al., 2000). The [ATP]-response curves for wild-type and C166S/N160D mutations (Fig. 2 *C*) are well fit by a Hill equation (solid lines):

$$\text{Irel} = (1 - C)(1/(1 + ([\text{ATP}]/K_{1/2})^{\text{H}})), \qquad (4)$$

where H = 1.2, 0.98 and $K_{1/2}$ = 8.1 μM, 966 μM, respectively (n = 3–6).

A non-zero plateau in the channel activity at saturating [ATP] is one possible prediction if ATP interacts with the open state, depending on the stability of the ATP-bound open state (see Discussion). As shown in Fig. 3 *A*, L164C is clearly very ATP insensitive and predicted to have a $K_{1/2,ATP} > 100$ mM (Fig. 3 *C*; Enkvetchakul et al., 2000) based on the assumption that full block would occur with a high enough [ATP]. However, this assumption cannot be tested because of the prohibitively high [ATP] needed, and a plateau in ATP inhibition could be missed. Based on an allosteric kinetic model (see below), the plateau in ATP inhibition may be predicted to occur at lower [ATP], i.e., in

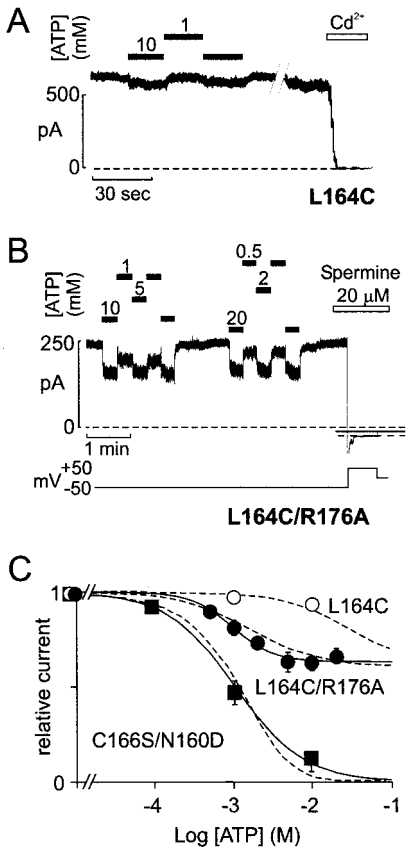

FIGURE 3 ATP inhibition has a non-zero plateau in the high open-state stability mutant L164C/R176A. (*A* and *B*) Representative recordings of L164C (*A*) and L164C/R176A (*B*) from inside-out membrane patches at −50 mV in K-INT solution, with application of ATP as indicated. Zero current was determined as either full block by cadmium (*A*) or by measuring leak current after full block with spermine at +50 mV membrane potential, using the voltage protocol indicated (*B*). (*C*) [ATP]-response relationships for the background C166S/N160D (■, taken from Fig. 2), L164C (○), and L164C/R176A (●). Solid lines represent Hill plots with offset; dashed lines are model predictions (see text).

a measurable range, by decreasing the channel-phosphatidylinositol bisphosphate (PIP_2) interaction. The mutation Kir6.2[R176A] has been shown to have a decreased PIP_2 interaction (Shyng and Nichols, 1998; Fan and Makielski, 1999) and was added to the L164C mutation to create the double mutant Kir6.2[L164C, R176A] (L164C/R176A), to examine this possibility.

The L164C/R176A mutant expresses K_{ATP} channels that are still Cd^{2+} sensitive (not shown) but which now have much higher apparent ATP sensitivity than L164C channels. ATP inhibition was measured in the double mutant L164C/R176A at six different ATP concentrations (Fig. 3 *B*), and zero current was estimated in the presence of 20 μM spermine at +50 mV. At ATP concentrations above 2 mM, inhibition becomes saturated at ~40% (Fig. 2 *B*). The [ATP]-response curve (Fig. 3 *C*) can be fitted by a Hill equation with an offset (solid line):

$$\text{Irel} = (1 - C)(1/(1 + ([\text{ATP}]/K_{1/2})^{H})) + C, \qquad (5)$$

where $H = 1.7$, $K_{1/2} = 950$ μM, and $C = 0.64$ ($n = 3$–5).

Open-time distributions are altered by ATP in L164C/R176A

Single-channel recordings of L164C/R176A were made in zero, 1, and 10 mM ATP (Figs. 4 and 5). Qualitatively similar results were obtained in several patches, and two patches were suitable for analysis in detail. Closed-time distributions show a characteristic fast peak (the fast flicker closure seen in all constructs) with $\tau = 0.22$ ms and a poorly resolved tail of longer closures. In the presence of ATP, this longer tail shifts slightly to the right, with an increase in frequency, reversible with removal of ATP (Fig. 5). Qualitatively, this behavior is quite similar to that previously recorded in wild-type and various mutant channels (Drain et al., 1998; Trapp et al., 1998; Enkvetchakul et al., 2000; Lin et al., 2000). Open-time distributions in the absence of ATP are mono-exponential, with $\tau = 2.3$ ms, again consistent with open times reported for various other Kir6.2 mutants and wild-type channels (Drain et al., 1998; Trapp et al., 1998; Enkvetchakul et al., 2000; Lin et al., 2000). However, in excised patches in the presence of ATP (Figs. 4 and 5), as well as in the on-cell configuration (Fig. 4), open-time distributions are markedly shifted to the left. Although there have been occasional reports of small left shifts in mean open time for other channel constructs with increasing [ATP], such a dramatic, reversible (Fig. 5), alteration in open-time distribution has not been reported.

ATP inhibition of M158C/R176A

The mutation Kir6.2[M158C] is also a relatively high open-probability mutant that is insensitive to ATP (Fig. 6 *A*), with an extrapolated $K_{1/2,ATP}$ of ~5 mM (Enkvetchakul et al., 2000) but again, the curve lies too far to the right to explore the possibility of a plateau of inhibition. We again added the mutation R176A, predicted to shift the ATP dose-response curve to the left (see below) and allow estimation of the full dose-response relationship. ATP inhibition was measured in M158C/R176A, with leak currents measured in the presence of 20 μM spermine at +50 mV membrane potential (Fig. 6 *B*). Again, complete inhibition does not occur, even at high [ATP], and a plateau is evident. Maximal inhibition by ATP is ~93%, with a small residual current even at the highest [ATP]. Steady-state [ATP]-response curves for M158C/R176A are fit by Eq. 5, with $H = 1.6$, $K_{1/2} = 242$ μM, and $C = 0.07$, $n = 4$ (Fig. 6 *C*).

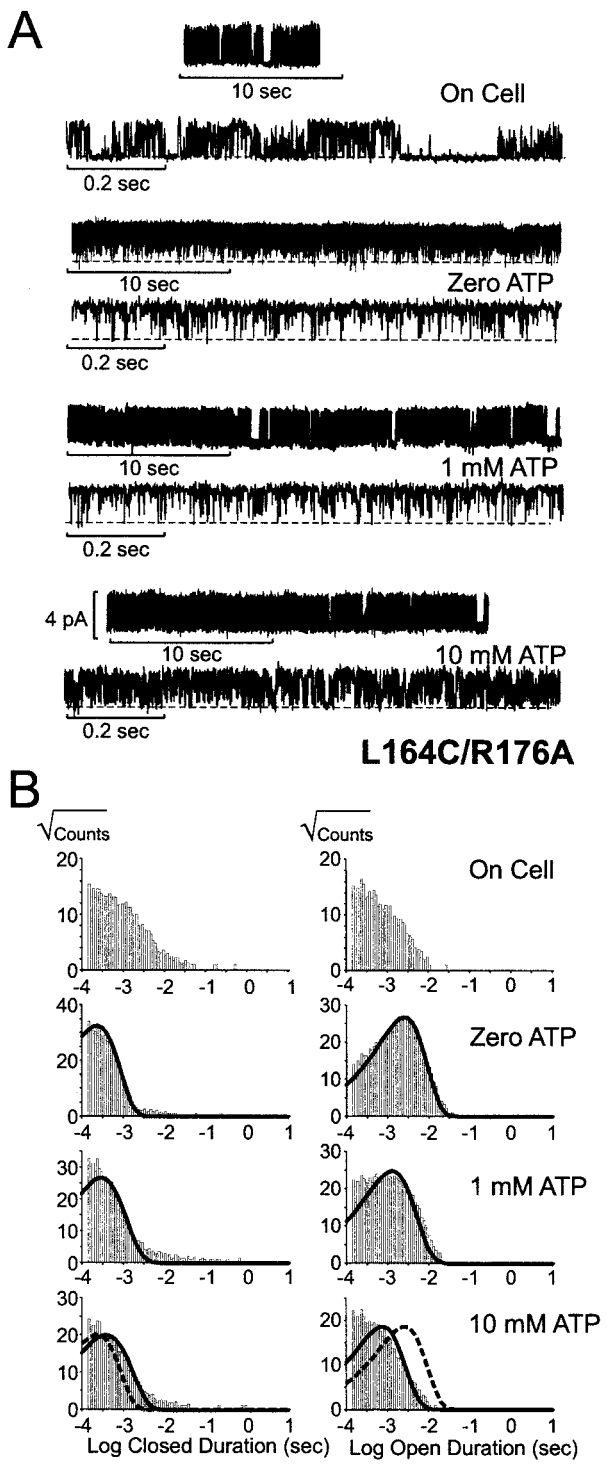

FIGURE 4 ATP alters open and closed time distributions in L164C/R176A. (*A*) Representative single-channel current of L164C/R176A recorded from a membrane patch on-cell and in inside-out mode at −50 mV membrane potential in symmetric K-INT solution. The patch was exposed to differing [ATP] and recordings are presented at two different time scales as indicated. (*B*) Sigworth-Sine histograms of open and closed events. Superimposed curves are probability density functions (PDFs) from simulations of model III (see text). Predicted PDFs in zero ATP are shown as dashed lines in the 10 mM ATP graph for comparison.

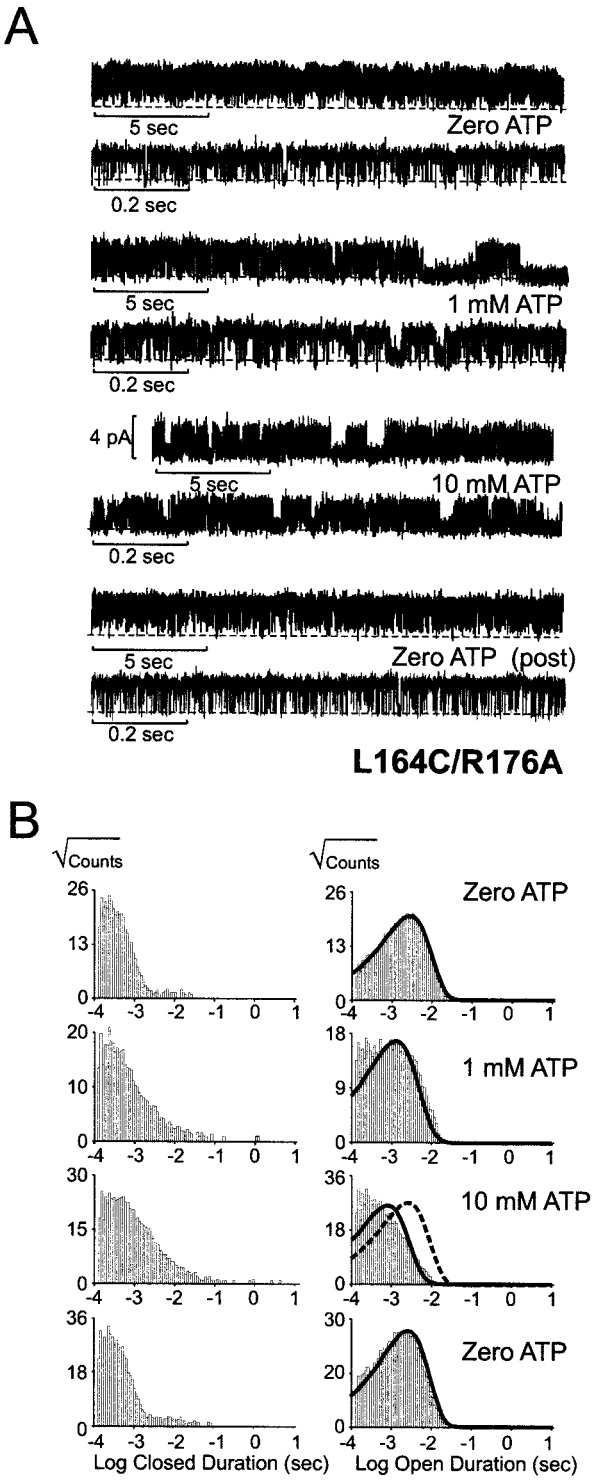

FIGURE 5 Shifts in open and closed time distributions in L164C/R176A by ATP are reversible. (*A*) Representative single-channel current of L164C/R176A recorded from another inside-out membrane patch at −50 mV membrane potential in symmetric K-INT solution. Patches were exposed to differing [ATP], and recordings are presented at two different time scales as indicated. (*B*) Sigworth-Sine histograms of open and closed events. Superimposed curves are simulations of PDFs from model III. The predicted open PDF in zero ATP is shown as a dashed line in the 10 mM ATP graph for comparison.

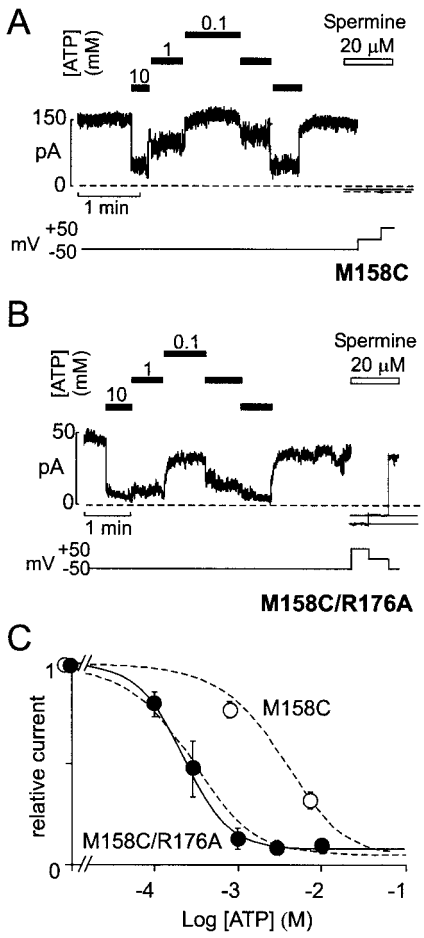

FIGURE 6 A non-zero plateau in ATP inhibition is seen in the high open-state stability mutant M158C/R176A. Representative recordings of M158C (*A*) and M158C/R176A (*B*) in inside-out patches at −50 mV membrane potential in K-INT solution, with application of ATP as indicated. Zero current was determined by measuring leak current after full block with spermine at +50 mV membrane potential, using voltage protocol shown. (*C*) ATP dose response of M158C (○) and M158C/R176A (●). Solid lines are Hill plots; dashed lines are from simulations of model III (see text).

DISCUSSION

ATP as an allosteric modulator of channel gating

Since the original description of K_{ATP} channel activity (Noma, 1983), it has been a long-held view that channel gating results from the binding of ATP to a gate that subsequently closes over the cytoplasmic entrance to the channel (Ashcroft, 1988; Nichols and Lederer, 1991). Nichols et al. (1991) suggested a four-state model in which a single ATP molecule was sufficient to close the channel, and subsequent ATP molecules, binding to each of the supposed four subunits of the channel, stabilized the closed state further. Since the cloning and recombinant expression of the relevant subunits (reviewed in Babenko et al., 1998), more complex models of nucleotide gating have been proposed (Shyng et al., 1997a; Alekseev et al., 1998; Trapp et al., 1998; Enkvetchakul et al., 2000; Lin et al., 2000). A few Kir6.2 mutations are known to alter ATP sensitivity without affecting the channel gating in the absence of ATP (Tucker et al., 1997; Li et al., 2000), but most mutations alter sensitivity to ATP inhibition ($K_{1/2,ATP}$) and open probability in the absence of ATP (P_{Ozero}) in a strongly correlated manner (Enkvetchakul et al., 2000). This correlation can be explained by assuming that ATP binds to, and hence stabilizes, the closed state (Shyng et al., 1997a; Enkvetchakul et al., 2000).

With no evidence for alterations in open-time distributions of these mutations in the presence of ATP, there has been no need to postulate an ATP-bound open state. Such evidence could come from demonstration of effects of ATP on open-time distributions, yet studies of mutant recombinant channels have generally demonstrated invariant open-time distributions (Alekseev et al., 1998; Drain et al., 1998; Trapp et al., 1998; Enkvetchakul et al., 2000). There have been sporadic reports of small, and variable, decreases in mean open times with ATP (Nichols et al., 1991; Fan and Makielski, 1999) and indirectly with increased glucose (assumed to increase [ATP]) (Ashcroft et al., 1986; Gillis et al., 1989; Cuevas et al., 1991) in both native and wild-type recombinant K_{ATP} channels. We now show clear evidence that ATP can interact with the open state of some mutant K_{ATP} channels. At a concentration that has no discernible inhibition of channel activity, ATP abolishes Cd^{2+} sensitivity of Kir6.2[L164C] + SUR1 (164C) channels. It might be conceivable that chelation of Cd^{2+} by ATP could prevent or halt Cd^{2+} inhibition. However, GTP, which is ineffective in gating K_{ATP} channels (Ashcroft, 1988; Nichols and Lederer, 1991), failed to prevent Cd^{2+} inhibition (data not shown). Moreover, recovery from Cd^{2+} inhibition by ATP could not be accounted for by chelation and can only be explained by ATP interaction with the Cd^{2+}-inhibited channel. Thus, it appears that ATP can bind to and conformationally affect the open, or Cd^{2+}-blocked, channel without causing closure. Accordingly, and in contrast to wild-type and low-open-state stability mutants, the L164C/R176A mutant shows two features of its behavior that provide direct evidence for ATP interaction with the open state, namely, a plateau in the ATP inhibition curve (Fig. 3) and significantly reduced open times in the presence of high [ATP] (Figs. 4 and 5).

Allosteric gating models for K_{ATP} channel

The strong correlation between $K_{1/2,ATP}$ and P_{Ozero} seen with a wide variety of mutations and with PIP_2 suggests a common mechanism affecting both. A kinetic model in which ATP interacts only with the closed channel can reproduce the effects of both M2 mutations and PIP_2 on the $K_{1/2,ATP}$–P_{Ozero} relationship, simply by assuming that these manipulations alter the open-closed transition equilibrium

(Enkvetchakul et al., 2000). In the model, each subunit can assume three separate states, and each subunit must be in the open state for the channel to conduct. Ignoring the distinct fast flicker-closures (but see Appendix), we may represent the model as:

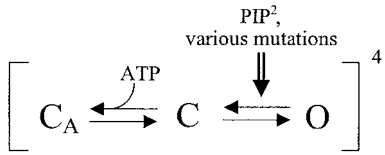

Model I

The critical transition (C↔ O) is affected by mutations in M2, and by PIP_2 (which shifts the equilibrium to the right). ATP accesses only the closed state of the subunit (C). The new data presented above clearly indicate that ATP can also interact with the open state, at least in some mutant channels. A simple extension of model I (in fact a generalization) leads to a model like that proposed for other allosteric proteins (Monod et al., 1965):

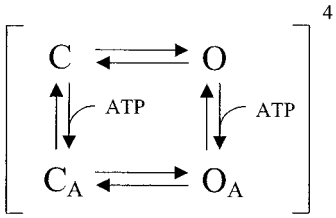

Model II

In this model, ATP can now be considered as an allosteric ligand that alters the equilibrium between open and closed states in each subunit. Again, the channel is assumed to have four identical subunits and is open only if all four are in an open state. PIP_2 can again be added as another allosteric ligand:

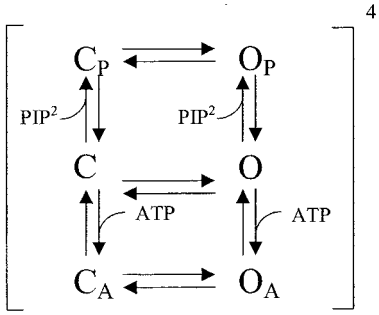

Model III

Predictions of this model III are shown in Fig. 7 and superimposed on the data in Figs. 2–6. Equilibrium constants (see Appendix) for wild type and for R176A were empirically selected to give $K_{1/2,ATP}$ of ~10 μM for both, and P_{Ozero} of 0.6 for wild type and <0.1 for R176A. The single assumption of the R176A mutation is a proportional decrease in the stability of the states C_P and O_P with respect to states C and O. The effects of M2 mutations are to cause shifts in the subunit closed-open equilibria. The dashed lines in Fig. 7 indicate the fraction of open channels with ATP bound to at least one subunit (i.e., subunits in the O_A state). For C166S/N160D mutant channels, there is a small window of [ATP] in which channels are predicted to be open with ATP bound. In the higher-open-state stability M158C and L164C mutations, this window becomes more prominent, and there is considerable steady-state occupancy at saturating [ATP]. Importantly, however, for both WT and R176A, states O_A and C_P are energetically so unfavorable that there is essentially no occupancy of these states at any [ATP], and the scheme can be simplified to model IIIa, in which ATP interacts only with the closed state, as in previous models (Shyng et al., 1997a; Enkvetchakul et al., 2000):

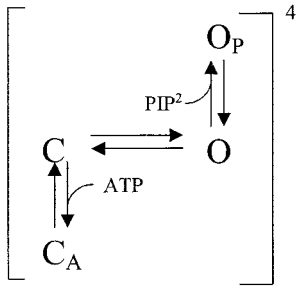

Model IIIa

The M2 mutations proportionally increase the stability of all open states (O_P, O, and O_A) with respect to the closed states (C_P, C, and C_A). In so doing, these mutations increase P_{Omax} and make the channel highly insensitive to ATP, and by causing significant occupancy of the O_A state, a plateau in inhibition is predicted at high [ATP]. By combining both stabilization of open states with respect to closed states (L164C or M158C), and destabilization of PIP_2-bound states (Op, Cp) with respect to all other states (R176A), the double mutations result in a leftward shift of the ATP dose-response curve and a plateau of inhibition within the experimentally accessible range of [ATP]. By making transition rates fast in the presence of ATP, the model predicts shortening of open times for these mutations in the presence of ATP (Figs. 4 and 5), as experimentally observed, although the multi-exponential nature of the L164C/R176A open-time distribution at high [ATP] is not particularly well reproduced.

Cd^{2+}-blocked states result from Cd^{2+} entry into the open pore. Can the model account for the effect of ATP on Cd^{2+} block? One potential explanation is to assume that the binding of ATP to the channel generates an insurmountable energetic barrier to Cd^{2+} entry or exit from the channel pore, so that there is no transition between ATP-bound open channels and ATP-bound, Cd^{2+}-blocked channels. Such a model would qualitatively replicate the essential findings of Fig. 1. As shown in Fig. 7 *C*, there is minimal channel

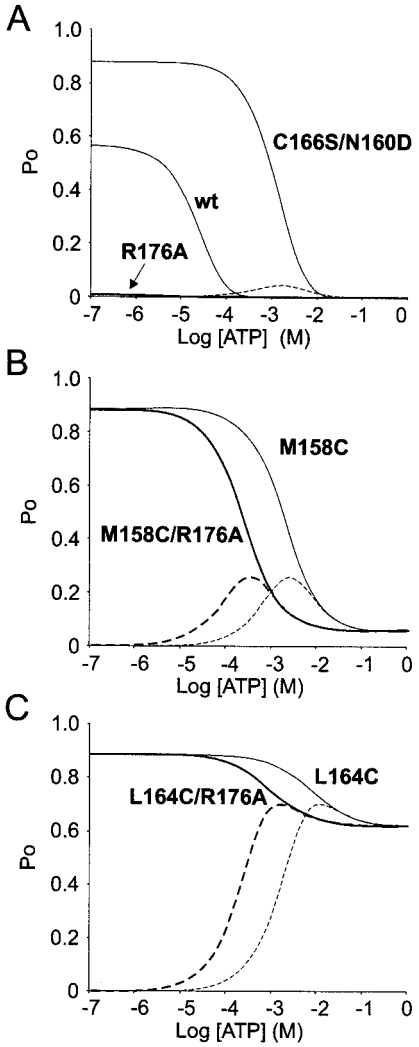

FIGURE 7 Simulation of [ATP]-response relationships using model III. (*A–C*) Solid lines represent the open probability of each channel; dashed lines represent fractional occupancy of open channels with one or more ATPs bound (see text).

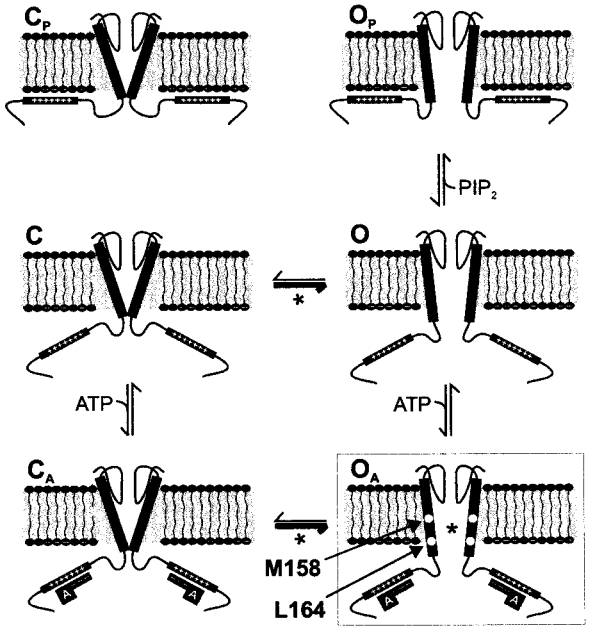

FIGURE 8 Cartoon illustrating an hypothesized physical basis of K_{ATP} channel gating: ATP and PIP_2 act as allosteric ligands. Channel opening and closing, associated with movement of the M2 helix, can occur with either ligand bound. However, for all channels, C_P is energetically unfavorable. The O_A state is also prohibitively unfavorable for the wild-type channel, such that the only route to closure is through unliganded states, and the closed state is then stabilized by ATP binding. The mutations L164C and M158C, both in the M2 domain, alter open-state stability by shifting all equilibria from closed to open states (indicated by asterisks), which then results in a significant occupancy of the ATP-bound open state.

inhibition, but a high fraction of ATP-bound open channels in L164C, at millimolar ATP. Thus, cadmium binding and release would be significantly slowed. Although this hypothesis is appealing, we have no speculation on a physical basis for such discrimination.

Parallel concepts for gating in the cation channel superfamily

Fig. 8 shows a cartoon representation of the possible physical basis of gating in K_{ATP} channels, which incorporates the kinetic scheme discussed above. The M2 segment is an α-helical segment that lines the inner vestibule of the channel (Doyle et al., 1998; Minor et al., 1999; Loussouarn et al., 2000), and the opening and closing of each subunit may involve motion of the M2 segment (Enkvetchakul et al., 2000). ATP and PIP_2 are envisioned as interacting in a mutually exclusive way (negative heterotropic cooperativity) with a positively charged region of the C-terminus and normally stabilizing the closed and open states, respectively (Enkvetchakul et al., 2000). The closed, PIP_2-bound state (C_P) is energetically unfavorable and essentially never accessed by any subunits. Mutations within the M2 region (e.g., M158C and L164C) affect the relative stabilities of open and closed states. Stabilization of the open state by these mutations, in particular by L164C, located at the lower end of M2, leads to increase in opening rate constants (asterisks) and significant, non-zero occupancy of the O_A state in the presence of ATP.

Recently, mutations in the voltage-gated Shaker K^+ channel P475D and P475E at the lower end of S6, analogous to the location of L164 at the lower end of M2, have been shown to have a non-zero minimum of open probability even at very negative membrane potentials (Hackos and Swartz, 2000), analogous to the pedestal seen with ATP in the L164C/R176A mutant. An additional report (Espinosa et al., 2000) on a voltage-gated K channel from *C. elegans* (EXP-2) indicates that bulky substitutions at another close residue (position 480) also induce a plateau of non-zero open probability at negative voltages. A common mecha-

TABLE 1 Subunit transition rate constants used in simulations (models III and IIIa)

$C_A \rightarrow O_A$ (s^{-1})	$O_A \rightarrow C_A$ (s^{-1})	$C \rightarrow O$ (s^{-1})	$O \rightarrow C$ (s^{-1})	$C_P \rightarrow O_P$ (s^{-1})	$O_P \rightarrow C_P$ (s^{-1})	$C_A \rightarrow C$ (μM^{-1} s^{-1})	$C \rightarrow C_A$ (s^{-1})
0.37*	370	6.4*	40	160*	1	1000	192
$O_A \rightarrow O$ (μM^{-1} s^{-1})	$O \rightarrow O_A$ (s^{-1})	$C_P \rightarrow C$ (s^{-1})	$C \rightarrow C_P$ (s^{-1})	$O_P \rightarrow O$ (s^{-1})	$O \rightarrow O_P$ (s^{-1})	$O \rightarrow C_f$ (s^{-1})	$C_f \rightarrow O$ (s^{-1})
1000	1.2	2000†	100	20†	1000	600	4500

Rate constants given are for wild-type Kir6.2 + SUR1 channels.
*Rate constants from C_P to O_P, from C to O, and from C_A to O_A were all increased 125-fold, 625-fold, or 7500-fold for the increased open-state stability mutants (control C166S/N160D, M158C, and L164C, respectively).
†Rate constants from O_P to O and from C_P to C were increased 30-fold for the mutant R176A (which decreases PIP_2 sensitivity).

nistic basis of gating, involving rotation and displacement of the S6 or M2 segments, proposed originally for KcsA (Perozo et al., 1999), seems increasingly likely for the gating of Kv channels (del Camino et al., 2000; Li-Smerin et al., 2000) and cyclic-nucleotide-gated channels (Flynn and Zagotta, 2000), and for inward rectifiers (Enkvetchakul et al., 2000; Loussouarn et al., 2000).

APPENDIX

For all simulations, it is assumed that the behavior of the channel as a whole depends on the ensemble behavior of four identical subunits, based on the knowledge that K_{ATP} channels are homotetramers (Aguilar-Bryan et al., 1995; Inagaki et al., 1995, 1996; Clement et al., 1997; Inagaki et al., 1997; Shyng and Nichols, 1997). Each subunit is also assumed to be kinetically independent; the whole channel is open, i.e., conducting, only if all four subunits are in an open state (open and closed subunit states are different from open and closed channels).

ATP dose-response curves were calculated by first determining the steady-state occupancy of the subunit. The steady-state probability for the channel assuming a particular combination of subunit states is then equal to the product of the steady-state occupancy of each subunit, multiplied by the number of distinguishable permutations possible for the given combination. For example, for model III, the probability that the channel had two subunits in the O state, and two in the C state, would equal 2 × (steady-state occupancy of O state) × 2 × (steady-state occupancy of closed state) × 4!/(2! × 2!). The channel open probability is then the sum of all possible open subunit combinations. Equilibria were assigned initally to approximate wild-type behavior (i.e., $K_{1/2,ATP} = \sim 10\ \mu M$, $P_{Ozero} = \sim 0.6$), resulting in the states C_P and O_A being energetically unfavorable. Mutations M158C and L164C were then assumed to increase open-state stability by proportionally shifting equilibria between closed and open states by the same ratio (see Table 1). Likewise, the mutation R176A was assumed to proportionally shift equilibria between PIP_2-bound and free states by a certain ratio.

For PDF calculations, each possible combination of the subunits was assumed to represent a unique state of the channel, with order of the subunits considered unimportant. Rate constants for transitions between states in each subunit were constrained by equilibria chosen above to simulate steady-state behavior. For the simulation of model III, there are a total of 126 unique combinations, 15 of which have all four subunits in an open state, and therefore the channel is open. An additional closed state was added off each open state to represent the fast flickering closures, for a total of 141 states. Transition pathways between these channel states were based on allowable transitions for each subunit, and rates between channel states were multiples of the transition rates for the subunit. Rate constants were adjusted with the above constraints to simulate single-channel open- and closed-time distributions for wild type (data not shown) and for L164C/R176A (see Table 1).

REFERENCES

Aguilar-Bryan, L., C. G. Nichols, S. W. Wechsler, J. P. Clement, I. V., A. E. Boyd, III, G. Gonzalez, H. Herrera-Sosa, K. Nguy, J. Bryan, and D. A. Nelson. 1995. Cloning of the beta cell high-affinity sulfonylurea receptor: a regulator of insulin secretion. *Science.* 268:423–426.

Alekseev, A. E., P. A. Brady, and A. Terzic. 1998. Ligand-insensitive state of cardiac ATP-sensitive K^+ channels: basis for channel opening. *J. Gen. Physiol.* 111:381–394.

Ashcroft, F. M. 1988. Adenosine 5′-triphosphate-sensitive potassium channels. *Annu. Rev. Neurosci.* 11:97–118.

Ashcroft, F. M., D. E. Harrison, and S. J. Ashcroft. 1986. A potassium channel modulated by glucose metabolism in rat pancreatic beta-cells. *Adv. Exp. Med. Biol.* 211:53–62.

Babenko, A. P., L. Aguilar-Bryan, and J. Bryan. 1998. A view of SUR/KIR6.X, K_{ATP} channels. *Annu. Rev. Physiol.* 60:667–687.

Clement, J. P., IV, K. Kunjilwar, G. Gonzalez, M. Schwanstecher, U. Panten, L. Aguilar-Bryan, and J. Bryan. 1997. Association and stoichiometry of K_{ATP} channel subunits. *Neuron.* 18:827–838.

Colquhoun, D., and A. G. Hawkes. 1995a. The Principles of the Stochastic Interpretation of Ion-Channel Mechanisms. *In* Single-Channel Recording. B. Sakmann and E. Neher, editors. Plenum Press, New York. 397–482.

Colquhoun, D., and A. G. Hawkes. 1995b. A Q-matrix cookbook: how to write only one program to calculate the single-channel and macroscopic predictions for any kinetic mechanism. *In* Single-Channel Recording. B. Sakmann and E. Neher, editors. Plenum Press, New York. 589–636.

Cuevas, J., A. L. Bassett, J. S. Cameron, T. Furukawa, R. J. Myerburg, and S. Kimura. 1991. Effect of H^+ on ATP-regulated K^+ channels in feline ventricular myocytes. *Am. J. Physiol.* 261:H755–H761.

del Camino, D., M. Holmgren, Y. Liu, and G. Yellen. 2000. Blocker protection in the pore of a voltage-gated K^+ channel and its structural implications. *Nature.* 403:321–325.

Doyle, D. A., J. Morais Cabral, R. A. Pfuetzner, A. Kuo, J. M. Gulbis, S. L. Cohen, B. T. Chait, and R. MacKinnon. 1998. The structure of the potassium channel: molecular basis of K^+ conduction and selectivity. *Science.* 280:69–77.

Drain, P., L. Li, and J. Wang. 1998. K_{ATP} channel inhibition by ATP requires distinct functional domains of the cytoplasmic C terminus of the pore-forming subunit. *Proc. Natl. Acad. Sci. U.S.A.* 95:13953–13958.

Enkvetchakul, D., G. Loussouarn, E. Makhina, S.-L. Shyng, and C. G. Nichols. 2000. The kinetic and physical basis of K(ATP) channel gating: toward a unified molecular understanding. *Biophys. J.* 78:2334–2348.

Espinosa, F., R. Fleischhauer, A. McMahon, M. W. Davis, L. Avery, and R. H. Joho. 2000. Bulky side-chain substitutions in S6 of EXP-2 trap the K^+ channel in an open state. *Biophys. J.* 78:271.

Fan, Z., and J. C. Makielski. 1999. Phosphoinositides decrease ATP sensitivity of the cardiac ATP-sensitive K^+ channel: a molecular probe for the mechanism of ATP-sensitive inhibition. *J. Gen. Physiol.* 114: 251–269.

Flynn, G. E., and W. N. Zagotta. 2000. Conformational changes in the S6 region of rod cyclic nucleotide-gated channels. *Biophys. J.* 78:148.

Gillis, K. D., W. M. Gee, A. Hammoud, M. L. McDaniel, L. C. Falke, and S. Misler. 1989. Effects of sulfonamides on a metabolite-regulated ATP-sensitive K^+ channel in rat pancreatic β-cells. *Am. J. Physiol.* 257:C1119–C1127.

Gribble, F. M., S. J. Tucker, and F. M. Ashcroft. 1997a. The essential role of the Walker A motifs of SUR1 in K-ATP channel activation by Mg-ADP and diazoxide. *EMBO J.* 16:1145–1152.

Gribble, F. M., S. J. Tucker, and F. M. Ashcroft. 1997b. The interaction of nucleotides with the tolbutamide block of cloned ATP-sensitive K^+ channel currents expressed in *Xenopus* oocytes: a reinterpretation. *J. Physiol. (Lond.).* 504:35–45.

Hackos, D. H., and K. J. Swartz. 2000. Mutations of a conserved proline in the inner helix of the pore domain of the Shaker K^+ channel with altered gating properties. *Biophys. J.* 78:398.

Inagaki, N., T. Gonoi, J. P. Clement, I. V., N. Namba, J. Inazawa, G. Gonzalez, L. Aguilar-Bryan, S. Seino, and J. Bryan. 1995. Reconstitution of IKATP: an inward rectifier subunit plus the sulfonylurea receptor. *Science.* 270:1166–1170.

Inagaki, N., T. Gonoi, J. P. Clement, I. V., C. Z. Wang, L. Aguilar-Bryan, J. Bryan, and S. Seino. 1996. A family of sulfonylurea receptors determines the pharmacological properties of ATP-sensitive K^+ channels. *Neuron.* 16:1011–1017.

Inagaki, N., T. Gonoi, and S. Seino. 1997. Subunit stoichiometry of the pancreatic beta-cell ATP-sensitive K^+ channel. *FEBS Lett.* 409: 232–236.

Isomoto, S., C. Kondo, M. Yamada, S. Matsumoto, O. Higashiguchi, Y. Horio, Y. Matsuzawa, and Y. Kurachi. 1996. A novel sulfonylurea receptor forms with BIR (Kir6.2) a smooth muscle type ATP-sensitive K^+ channel. *J. Biol. Chem.* 271:24321–24324.

Li, L., J. Wang, and P. Drain. 2000. The I182 region of Kir6.2 is closely associated with ligand binding in K_{ATP} channel inhibition by ATP. *Biophys. J.* 79:841–852.

Lin, Y. F., Y. N. Jan, and L. Y. Jan. 2000. Regulation of ATP-sensitive potassium channel function by protein kinase A-mediated phosphorylation in transfected HEK293 cells. *EMBO J.* 19:942–955.

Li-Smerin, Y., D. H. Hackos, and K. J. Swartz. 2000. A localized interaction surface for voltage-sensing domains on the pore domain of a K^+ channel. *Neuron.* 25:411–423.

Loussouarn, G., E. N. Makhina, T. Rose, and C. G. Nichols. 2000. Structure and dynamics of the pore of inwardly rectifying K_{ATP} channels. *J. Biol. Chem.* 275:1137–1144.

Minor, D. L., Jr., S. J. Masseling, Y. N. Jan, and L. Y. Jan. 1999. Transmembrane structure of an inwardly rectifying potassium channel. *Cell.* 96:879–891.

Monod, J., J. Wyman, and J.-P. Changeux. 1965. On the nature of allosteric transitions: a plausible model. *J. Mol. Biol.* 12:88–118.

Nichols, C. G., and W. J. Lederer. 1991. Adenosine triphosphate-sensitive potassium channels in the cardiovascular system. *Am. J. Physiol.* 261: H1675–H1686.

Nichols, C. G., W. J. Lederer, and M. B. Cannell. 1991. ATP dependence of K_{ATP} channel kinetics in isolated membrane patches from rat ventricle. *Biophys. J.* 60:1164–1177.

Nichols, C. G., S.-L. Shyng, A. Nestorowicz, B. Glaser, J. P. Clement, I. V., G. Gonzalez, L. Aguilar-Bryan, M. A. Permutt, and J. Bryan. 1996. Adenosine diphosphate as an intracellular regulator of insulin secretion. *Science.* 272:1785–1787.

Noma, A. 1983. ATP-regulated K^+ channels in cardiac muscle. *Nature.* 305:147–148.

Perozo, E., D. M. Cortes, and L. G. Cuello. 1999. Structural rearrangements underlying K^+-channel activation gating. *Science.* 285:73–78.

Qin, F., A. Auerbach, and F. Sachs. 1996. Estimating single-channel kinetic parameters from idealized patch-clamp data containing missed events. *Biophys. J.* 70:264–280.

Schwanstecher, M., C. Sieverding, H. Dorschner, I. Gross, L. Aguilar-Bryan, C. Schwanstecher, and J. Bryan. 1998. Potassium channel openers require ATP to bind to and act through sulfonylurea receptors. *EMBO J.* 17:5529–5535.

Shyng, S.-L., T. Ferrigni, and C. G. Nichols. 1997a. Control of rectification and gating of cloned K_{ATP} channels by the Kir6.2 subunit. *J. Gen. Physiol.* 110:141–153.

Shyng, S.-L., T. Ferrigni, and C. G. Nichols. 1997b. Regulation of K_{ATP} channel activity by diazoxide and MgADP: distinct functions of the two nucleotide binding folds of the sulfonylurea receptor. *J. Gen. Physiol.* 110:643–654.

Shyng, S.-L., and C. G. Nichols. 1997. Octameric stoichiometry of the K_{ATP} channel complex. *J. Gen. Physiol.* 110:655–664.

Shyng, S.-L., and C. G. Nichols. 1998. Membrane phospholipid control of nucleotide sensitivity of K_{ATP} channels. *Science.* 282:1138–1141.

Tanabe, K., S. J. Tucker, M. Matsuo, P. Proks, F. M. Ashcroft, S. Seino, T. Amachi, and K. Ueda. 1999. Direct photoaffinity labeling of the Kir6.2 subunit of the ATP- sensitive K^+ channel by 8-azido-ATP. *J. Biol. Chem.* 274:3931–3933.

Tibbs, G. R., E. H. Goulding, and S. A. Siegelbaum. 1997. Allosteric activation and tuning of ligand efficacy in cyclic-nucleotide-gated channels. *Nature.* 386:612–615.

Trapp, S., P. Proks, S. J. Tucker, and F. M. Ashcroft. 1998. Molecular analysis of ATP-sensitive K channel gating and implications for channel inhibition by ATP. *J. Gen. Physiol.* 112:333–349.

Tucker, S. J., F. M. Gribble, P. Proks, S. Trapp, T. J. Ryder, T. Haug, F. Reimann, and F. M. Ashcroft. 1998. Molecular determinants of K_{ATP} channel inhibition by ATP. *EMBO J.* 17:3290–3296.

Tucker, S. J., F. M. Gribble, C. Zhao, S. Trapp, and F. M. Ashcroft. 1997. Truncation of Kir6.2 produces ATP-sensitive K^+ channels in the absence of the sulphonylurea receptor. *Nature.* 387:179–183.